Mechanistic Characterization of the HDV Genomic Ribozyme: Classifying the Catalytic and Structural Metal Ion Sites within a Multichannel Reaction Mechanism†

Shu-ichi Nakano,‡ Andrea L. Cerrone, and Philip C. Bevilacqua*

Department of Chemistry, The Pennsylvania State University, University Park, Pennsylvania 16802

Received September 7, 2002; Revised Manuscript Received January 6, 2003

ABSTRACT: Prior studies of the metal ion dependence of the self-cleavage reaction of the HDV genomic ribozyme led to a mechanistic framework in which the ribozyme can self-cleave by multiple Mg^{2+} ion-independent and -dependent channels [Nakano et al. (2001) *Biochemistry 40*, 12022]. In particular, channel 2 involves cleavage in the presence of a structural Mg^{2+} ion without participation of a catalytic divalent metal ion, while channel 3 involves both structural and catalytic Mg^{2+} ions. In the present study, experiments were performed to probe the nature of the various divalent ion sites and any specificity for Mg^{2+}. A series of alkaline earth metal ions was tested for the ability to catalyze self-cleavage of the ribozyme under conditions that favor either channel 2 or channel 3. Under conditions that populate primarily channel 3, nearly identical K_ds were obtained for Mg^{2+}, Ca^{2+}, Ba^{2+}, and Sr^{2+}, with a slight discrimination against Ca^{2+}. In contrast, under conditions that populate primarily channel 2, tighter binding was observed as ion size decreases. Moreover, $[Co(NH_3)_6]^{3+}$ was found to be a strong competitive inhibitor of Mg^{2+} for channel 3 but not for channel 2. The thermal unfolding of the cleaved ribozyme was also examined, and two transitions were found. Urea-dependent studies gave *m*-values that allowed the lower temperature transition to be assigned to tertiary structure unfolding. The effects of high concentrations of Na^+ on the melting temperature for RNA unfolding and the reaction rate revealed ion binding to the folded RNA, with significant competition of Na^+ (Hill coefficient of $\approx$1.5−1.7) for a structural Mg^{2+} ion and an unusually high intrinsic affinity of the structural ion for the RNA. Taken together, these data support the existence of two different classes of metal ion sites on the ribozyme: a structural site that is inner sphere with a major electrostatic component and a preference for Mg^{2+}, and a weak catalytic site that is outer sphere with little preference for a particular divalent ion.

Metal ions play a variety of roles in the folding of complex RNA structures and in the catalytic activity of ribozymes. Divalent ions have long been recognized as necessary for the tertiary folding of RNA under physiological ionic strengths. For example, yeast $tRNA^{Phe}$ requires 3−6 Mg^{2+} ions for proper tertiary folding at low ionic strength (*1*−*3*), and pseudoknots typically require delocalized divalent metal ions to fold efficiently (*4*, *5*). One of the primary reasons divalent metal ions are required is to neutralize the close approach of negatively charged phosphates that occurs upon compaction of the RNA molecule. Metal ions can be thermodynamically bound at specific sites, "site bound", or kinetically labile, "diffuse" or "delocalized" (*6*). In addition, site-bound metal ions can remain fully hydrated, "outer sphere", or can become partially or fully dehydrated, "inner sphere" (*6*). Monovalent ions have also been shown to play important roles in both the secondary and tertiary folding of RNAs. For example, high concentrations of monovalent ions, typically 0.1 M or greater, can induce the proper tertiary folding of many RNAs (*6*), and monovalent ions can be site bound, with several examples of dehydrated K^+ ions known (*7*−*9*).

The ribozyme from hepatitis delta virus (HDV)[1] occurs in closely related genomic and antigenomic forms (*10*), and a crystal structure is available for the cleaved form of the genomic ribozyme (*11*, *12*). The ribozyme adopts a complex tertiary structure involving nested pseudoknots and a buried active site. The ribozyme can accelerate the rate of cleavage of a phosphodiester bond between positions −1 and +1 and gives 5′-hydroxyl and 2′,3′-cyclic phosphate termini. The mechanism for self-cleavage provided an example of general acid−base catalysis by a ribozyme (*13*, *14*), and general acid−base catalysis has subsequently been suggested in the mechanisms of the ribosome (*15*) and the hairpin ribozyme (*16*). A cytosine residue (C75 in the genomic ribozyme, C76 in the antigenomic ribozyme) near the scissile bond has been shown by kinetic studies to have a pK_A near neutrality (*13*,

† Supported by NIH Grant GM58709 and a Camille Dreyfus Teacher−Scholar Award and Sloan Fellowship to P.C.B.

* To whom correspondence should be addressed. Phone: (814) 863-3812. Fax: (814) 863-8403. E-mail: pcb@chem.psu.edu.

‡ Current address: High Technology Research Center, Konan University, 8-9-1 Okamoto, Higashinada-ku, Kobe 658-8501, Japan.

[1] Abbreviations: AS(−30/−7), antisense oligomer complementary to nucleotides −30 to −7; EDTA, ethylenediaminetetraacetic acid; HEPES, 4-(2-hydroxyethyl)-1-piperazineethanesulfonic acid; G11C, ribozyme used in these studies with a G to C change at position 11; HDV, hepatitis delta virus; PAGE, polyacrylamide gel electrophoresis; TE, 10 mM Tris and 1 mM EDTA (pH 7.5); TEN_{250}, TE with 250 mM NaCl; Tris, tris(hydroxymethyl)aminomethane; UV, ultraviolet.

10.1021/bi026815x CCC: $25.00
Published on Web 02/22/2003

Scheme 1: Proposed Proton Transfers in Bond Cleavage

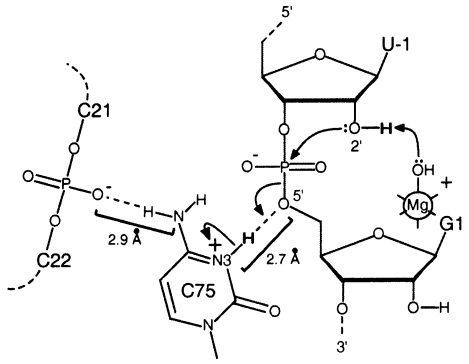

14) and has been implicated as the general acid in the reaction, acting to protonate the 5′-bridging oxygen (*14*, *17*, *18*) (Scheme 1). NMR studies provided evidence that this pK_A is not shifted in the product form of the ribozyme, suggesting that it may shift in the transition state or in a high-energy ground state of a properly folded precursor ribozyme (*19*).

A pentahydrated metal hydroxide has been implicated as the general base in the reaction under near-physiological metal ion conditions to deprotonate the 2′-OH nucleophile (*14*, *20*) (Scheme 1). Additionally, proton inventory studies provided evidence for two proton transfers in the reaction (*17*). Brønsted studies of exogenous base rescue of a C76-deleted antigenomic ribozyme indicated that approximately half of this proton is transferred in the transition state (*21*); likewise, Brønsted studies of the metal dependence of the reaction for the genomic ribozyme indicated that half of a proton is transferred to the general base in the transition state (*20*). α- and *β*-values similar to these have been found for cleavage of RNA by the protein enzyme, RNase A (*22*).

To assess the contributions of metal ions to folding and catalysis in the HDV genomic ribozyme, we examined self-cleavage over a wide range of Mg^{2+} ion concentrations using a metal-buffered system in the presence of high ionic strength (1 M NaCl) (*20*). The data could be described with a multichannel kinetic model in which each channel involved a different role for Mg^{2+} ions. Multichannel models have subsequently been applied to the hammerhead ribozyme (*23*). Surprisingly, the HDV ribozyme was found to cleave in the absence of participating divalent metal ions (channel 1), indicating that divalent ions are not absolutely necessary for folding or catalysis of the ribozyme (*14*, *20*). Channel 2 of the mechanism involves a structural Mg^{2+} ion, while channel 3 involves both structural and catalytic Mg^{2+} ions. Assessment of the contributions of these ions to the rate of cleavage in 1 M ionic strength gave ≈125-fold for the structural ion and only ≈25-fold for the catalytic ion (*20*). However, these studies did not provide insight into the nature of the divalent metal ion sites or any specificity toward Mg^{2+}.

In an effort to characterize the divalent metal ion sites, we have probed the effect of changing the metal ion under conditions that populate primarily channel 2 or channel 3. We used a series of mono-, di-, and trivalent metal ions at various concentrations and measured their effects on catalysis and RNA unfolding thermodynamics. Our data support two different classes of metal ion sites on the HDV ribozyme: an inner-sphere structural site and an outer-sphere catalytic site.

Scheme 2: Three-Channel Mechanism for Ribozyme Cleavage

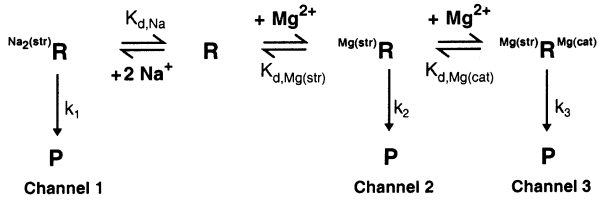

MATERIALS AND METHODS

Materials. Unless otherwise noted, the ribozyme and solutions were prepared, and the RNA was renatured as described (*20*, *24*). All experiments used the G11C mutant of the −30/99 ribozyme which leads to fast monophasic folding due to destabilization of the Alt P1 misfold (*25*). Reactions were promoted with the AS(−30/−7) antisense oligonucleotide, which acts to resolve the Alt 1 misfold (*24*), and were initiated by addition of divalent ion or a divalent ion/Na^+ mixture, as appropriate.

Kinetic Methods and Data Fitting. In general, kinetics methods followed those previously described (*20*). Plots of cleavage rate versus divalent ion concentration were fit to linear or logarithmic versions of the Hill equation (eq 1a,b)

$$k_{obs} = \frac{k_{max}[M]^{\alpha_H}/K_d^{\alpha_H}}{1 + [M]^{\alpha_H}/K_d^{\alpha_H}} \quad (1a)$$

$$\log\frac{k_{max} - k_{obs}}{k_{obs}} = -\alpha_H \log [M] + \alpha_H \log K_d \quad (1b)$$

where [M] is the concentration of a given ion, k_{obs} is the observed rate constant, k_{max} is k_{obs} at saturating ion concentrations, α_H is the Hill constant, which is a lower limit for the number of ions taken up by the RNA, and K_d is the apparent dissociation constant for ion binding to the RNA.

Data for the three-channel model were fit according to Scheme 2, with three linked equilibria. Binding of the structural and catalytic Mg^{2+} ions is shown as sequential on the basis of previous studies (*20*), and the binding of the two Na^+ ions is treated as cooperative, although the Hill coefficient reveals a measure of actual cooperativity.

k_{obs} is the weighted sum of the rate constants for each channel

$$k_{obs} = k_1 f_1 + k_2 f_2 + k_3 f_3 \quad (2)$$

where the weight for channel i is f_i, the fractional occupancy. The fractional occupancy of each channel is defined in terms of the partition function, Q

$$Q = 1 + \frac{[Na^+]^2}{K_{d,Na^+}^2} + \frac{[Mg^{2+}]}{K_{d,str}} + \frac{[Mg^{2+}]^2}{K_{d,str}K_{d,cat}} \quad (3)$$

so that

$$f_1 = \frac{[Na^+]^2/K_{d,Na^+}^2}{Q} \quad (4a)$$

$$f_2 = \frac{[Mg^{2+}]/K_{d,str}}{Q} \quad (4b)$$

$$f_3 = \frac{[Mg^{2+}]^2/K_{d,str}K_{d,cat}}{Q} \quad (4c)$$

Thus, in the absence of Mg^{2+}

$$k_{obs} = \frac{k_1[Na^+]^2/K^2_{d,Na^+}}{1 + [Na^+]^2/K^2_{d,Na^+}} \quad (5)$$

and when $[Na^+] \ll K_{d,Na^+}$

$$\log k_{obs} \approx 2 \log [Na^+] + \log(k_1/K^2_{d,Na^+}) \quad (6)$$

and the slope of the steep portion of a log k_{obs} versus log $[Na^+]$ plot should approach 2 when the binding of the sodium ions is cooperative.

Likewise, under Mg^{2+} concentrations wherein channel 2 dominates the reaction ($k_2 \gg k_1$; see Results and Discussion).

$$k_{obs} = \frac{k_2[Mg^{2+}]/K_{d,str}}{1 + \dfrac{[Na^+]^2}{K^2_{d,Na^+}} + \dfrac{[Mg^{2+}]}{K_{d,str}}} \quad (7)$$

Therefore, this leads to a $K_{d,app}$ of

$$K_{d,app} = K_{d,str}(1 + [Na^+]^2/K^2_{d,Na^+}) \quad (8)$$

which is of the form expected for cooperative binding of two Na^+ ions competitively inhibiting binding of one structural Mg^{2+} ion.

The equations from the kinetic model for Scheme 2 were derived with the assumption that the three channels are in rapid equilibrium. There are several observations that support this. (A) Metal ions typically bind rapidly to nucleic acids, and their translation along a nucleic acid has no significant barrier (*6*). Of course, binding of a metal ion to a final folded state can appear slow if binding either requires or induces a conformational change of the RNA with a significant barrier. However, the experiments herein involving Na^+ competition were done in 1 M NaCl such that the ribozyme should be largely prefolded into the correct conformation. (B) Binding constants for the inner- and outer-sphere metal ions are similar to those expected from the literature, as pointed out in the text. (C) Binding constants for the inner-sphere metal ion inferred from cleavage studies are in good agreement with those from melting experiments. Nevertheless, we do not have proof that channels are all in rapid equilibrium. As such, binding constants for metal ions should be viewed as apparent.

Thermodynamic Methods and Data Fitting. The RNAs used in UV melting studies were of the self-cleaved G11C ribozyme from +1 to 99. This species was prepared by allowing the ribozyme to react to completion in the presence of AS(−30/−7) and Mg^{2+} (*24*). Cleaved RNAs were purified by denaturing 5% PAGE and eluted in TEN_{250}. The RNA was ethanol precipitated, washed with 70% ethanol, and stored in TE at −20 °C.

Scheme 3

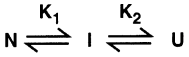

UV melting profiles were obtained at 260 nm on a Gilford Response II spectrophotometer, using a 0.5 cm cuvette and 0.1−0.5 μM RNA. The RNA was renatured prior to melting as described (*24*). Representative samples were melted at 0.1 and 0.5 μM, and identical results were obtained, consistent with melting of a monomeric RNA species. Heating and cooling curves were superimposable in both Na^+ and Mg^{2+} (for pH 7.0 melts), consistent with reversibility and thermodynamic equilibrium. The heating rate was approximately 1 °C/min, and the data were smoothed over five points before the first derivative of absorbance was calculated with respect to temperature. First derivatives were normalized by dividing by the absorbance at the lowest temperature after smoothing (*26*). (Low temperature was chosen since absorbance at high temperature can reflect differences in hydrolysis of the RNA backbone, especially in the presence of divalent ions.) The buffer was 25 mM HEPES (pH 7.0) (or pH 8.0 for urea dependence experiments), and the pH was adjusted at room temperature. At pH 8.0, only forward melts were used due to hydrolysis at high temperatures.

Melting of the cleaved ribozyme revealed two unfolding transitions which were consistent with unfolding of tertiary and secondary structure (see Results and Discussion). In an effort to obtain thermodynamic parameters for the transitions, the data were fit to linked equilibria for a sequential unfolding model (Scheme 3) involving native (N), intermediate (I), and unfolded (U) species; these appear to correspond to tertiary, secondary, and primary structure, respectively.

In general, the data were fit according to the methods of Draper, Giedroc, and co-workers (*5*, *26*, *27*). Scheme 3 can be described with a partition function of

$$Q = 1 + K_1 + K_1K_2 \quad (9)$$

and the absorbance can be defined as the sum of ΔA_t and B

$$\Delta A_t = \frac{\Delta A_1 K_1}{Q} + \frac{(\Delta A_1 + \Delta A_2)K_1K_2}{Q} \quad (10)$$

$$B = B_N + \left(\frac{B_U - B_N}{\Delta H_1 + \Delta H_2}\right)\left(\frac{\Delta H_1 K_1 + (\Delta H_1 + \Delta H_2)K_1K_2}{Q}\right) \quad (11)$$

ΔA_t is the total hyperchromicity, and ΔA_1 and ΔA_2 are the fractional hyperchromicities for transitions 1 and 2. B is a baseline function, and B_U and B_N are the sloping lines for the upper and lower baselines, respectively, with the intermediate treated with an enthalpy-weighted baseline. The slopes and intercepts of the upper and lower baselines were determined independently by linear least-squares fits of the low- and high-temperature portions of the data and were held constant during the actual fit. The baselines were chosen to minimize χ^2 of the fit. Thus, only six parameters were adjusted in the fit, namely, $\Delta H°$, T_M, and ΔA for the first and second transitions. $\Delta H°_i$ and $T_{M,i}$ for the ith transition were determined from the van't Hoff relationship

$$K_i = \exp\left[\frac{\Delta H_i}{R}\left(\frac{1}{T_{M,i}} - \frac{1}{T}\right)\right] \quad (12)$$

where R is the ideal gas constant and T is absolute temperature. Curve fitting of absorbance versus temperature data was to the sum of eqs 10 and 11, with Q, B_U, B_N, K_1, and K_2 defined parametrically using Kaleidagraph v3.5 (Synergy Software). ΔS_i was obtained from $T_{M,i} = \Delta H_i/\Delta S_i$, and $\Delta G_{37,i}$ was from $\Delta G_{37,i} = \Delta H_i - 310.15\Delta S_i$.

The m-value of the ith transition, m_i, was calculated as the slope of a $\Delta G_{37,i}$(urea) versus urea concentration plot on the basis of the relationship

$$\Delta G_{37,i}(\text{urea}) = \Delta G_{37,i} + m_i[\text{urea}] \quad (13)$$

where $\Delta G_{37,i}$(urea) is the observed free energy for transition i at a given urea concentration and m_i is a thermodynamic parameter that describes the dependence of free energy on urea concentration (*28*).

The dependence of T_M on metal ion concentration was analyzed according to the formalism previously developed (*5*, *27*, *29*). Briefly, a set of coupled equilibria was used in which all possible ligand-bound forms of the folded (F) and unfolded (U) RNAs involved in a two-state transition are considered. (Note that we consider the simple two-state F ↔ U transition and later extend this to Scheme 3.) The observed equilibrium constant for unfolding (K_{obs}) is then

$$\ln K_{obs} = \ln K_o + \ln \Sigma_u - \ln \Sigma_f \quad (14)$$

where K_o is the observed equilibrium constant in the absence of the ligand and Σ_u and Σ_f are binding polynomials for the unfolded and folded states, respectively. A useful form of this equation can be reached by applying the van't Hoff equation in the absence of ligand, using T_0, the T_M in the absence of the ligand, and T_L, the T_M at ligand concentration L

$$1/T_L = 1/T_0 - R/\Delta H_0 \ln(\Sigma_f/\Sigma_u) \quad (15)$$

where ΔH_0 is the unfolding enthalpy in the absence of ligand. As described by Laing and co-workers (*27*), the functional forms of Σ_u and Σ_f depend on whether the metal ions bind to F only or to both F and U. If the ions bind nonspecifically to F and U, then plots of $1/T_L$ versus ln [L] are expected to be sigmoidal; however, if binding is specific to F, such plots are expected to decrease indefinitely with metal ion concentration at high metal ion concentrations and have a slope of $-n_F R/\Delta H_0$, where n_F is the number of ions bound to F (*27*).

$$\frac{d(1/T_L)}{d(\ln [L])} = -n_F\left(\frac{R}{\Delta H_0}\right) \quad (16)$$

For this equation, the enthalpies for ion binding to the folded and unfolded states, ΔH_f and ΔH_u, are assumed to be zero. As described, this assumption can introduce small errors in some instances (*27*).

The case of ion binding to F only appears to apply to our data. Fortunately, under these conditions, Σ_u can be considered to be unity. For specific binding of Mg^{2+} to independent sites on F

$$\Sigma_f = (1 + K_f[Mg^{2+}])^{n_F} \quad (17)$$

where K_f is the association constant for Mg^{2+} binding to the native RNA. Note that this model does not take into account any cooperativity (positive or negative) between binding of multiple ions.

This formalism was developed for the two-state transition of F ↔ U. For a three-state system (Scheme 3), these equations can still be applied to one of the two transitions if that transition is well isolated from the other or if the data are treated with coupled equilibria. For our purposes, $1/T_L$ for the first transition in Scheme 3 was plotted versus metal ion concentration and fit to eq 15 with $\Sigma_I = 1$ and Σ_N as defined in eq 17.

It should be noted that for the urea dependence experiments an upper baseline could be reasonably well defined, allowing thermodynamic parameters for both transitions to be obtained. However, with increasing Na^+ and Mg^{2+} concentrations in the absence of urea, the extraordinary stability of the ribozyme precluded a good upper baseline from being obtained. In these cases, T_L of the first transition was estimated from the maximum of the first derivative; this appears reasonable since the maxima of the two transitions were well-resolved even at high ligand concentration.

It is worth pointing out the connection between Schemes 2 and 3. N in Scheme 3 refers collectively to all four states involving R in Scheme 2, and the states involving I and U are not shown explicitly since the kinetic experiments were at temperatures well below the T_M for N. However, as pointed out in the text, states involving I may be important in the kinetic mechanism, especially in monovalent ions (*20*), since the precursor ribozyme may have more unfavorable interactions than the cleaved ribozyme. Implications for this possibility are considered in the text.

BACKGROUND

Analysis of the binding of metal ions to nucleic acids is complicated by the wide variety of ion sites and binding modes possible, some of which obey mass action and some of which do not (e.g., diffuse ions). Moreover, if the specific ion-free state of the RNA does not have tertiary structure, the contributions of ions to site binding and to folding are typically coupled, leading to the highly cooperative binding of multiple ions (*6*). This scenario makes classification of the mode of binding of a few structural or catalytic ions difficult, if not impossible. In contrast, binding of ions of RNAs with preformed tertiary structure at high monovalent salt concentrations is typically noncooperative, allowing the opportunity to characterize the mode of ion binding (*6*). Thus, it is imperative to identify solution conditions under which an RNA molecule is largely folded and the filling of only a few metal ion sites occurs.

Experiments for the genomic HDV ribozyme conducted with metal-buffered solutions in 1 M NaCl (*20*) suggested conditions that might be tried for examining the structural and catalytic metal ions separately. Conditions were sought for which small Hill coefficients occur for filling the structural or catalytic site. For probing the structural site, this condition was fulfilled by reaction conditions under which channel 2 dominates and the catalytic ion is not involved. In particular, conditions of 1 M NaCl and pH 7.0 were found to give divalent ion binding isotherms well described with an α_H of 1, suggesting binding of one structural ion (*20*). In contrast, raising the pH to 8.0 in 1 M

NaCl increased the affinity of the catalytic ion and decreased the affinity of the structural ion such that distinctly cooperative binding behavior was observed with an α_H of 1.85 (*20*). This was interpreted in terms of a model in which a structural Mg^{2+} ion is ≈125-fold more effective than NaCl (even at a concentration of 1 M) at stabilizing the functional tertiary structure, and the catalytic ion binds only to the folded tertiary structure (see sequential ion binding model in Scheme 2) (*20*). Of practical relevance to the studies here, conditions of 1 M NaCl and pH 7.0 seemed optimal for testing the nature of the structural metal ion. Results with various divalent metal ions and $Co(NH_3)_6^{3+}$ support this notion (see below).

For probing the catalytic site, the α_H of unity condition was fulfilled by keeping the structural site saturated at all metal ion concentrations tested. Since the structural site is competitively inhibited by Na^+ (see below), this was achieved with a background of low ionic strength. At low ionic strength, an additional concern becomes the occurrence of bulk electrostatic effects in which multiple ions bind simultaneously to induce correct folding of an RNA (*6*). For tRNA, which is similar in size and buried surface area to the HDV ribozyme (*9*), these ions bind with K_ds of 100−170 μM under ionic strengths similar to those used in Figure 1A (*6*). The K_ds observed herein are 10−50 times weaker than this value (Figure 1A, Table 1), suggesting that both specific and nonspecific ions are largely associated with the RNA before the onset of binding in Figure 1A. Moreover, previous studies under these conditions provided evidence that binding of one Mg^{2+} ion and one H^+ ion to C75 of the ribozyme is negatively linked and that this Mg^{2+} ion inverts the pH profile of the reaction (*14*, *20*). Collectively, these data suggest that rate profiles obtained under low ionic strength conditions are not dominated by bulk electrostatic effects and that these conditions probe the catalytic metal ion.

RESULTS AND DISCUSSION

Metal Ion Dependence Supports an Outer-Sphere Site for the Catalytic Ion. As described in the Background section, we probed the catalytic ion under conditions of low ionic strength. The first experiments examined the effect of changing Mg^{2+} to other group IIA metal ions. As shown in Figure 1A, Mg^{2+}, Ca^{2+}, Sr^{2+}, and Ba^{2+} gave binding isotherms that were well described with an α_H of 1, resulting in similar K_d values of 2.4, 4.8, 2.7, and 1.2 mM, respectively (Table 1). Binding was weakest for Ca^{2+} and tightest for Ba^{2+} but does not show a monotonic dependence on ionic radius or a large dynamic range in K_d values (Figure 1C) (compare to structural site below). Prior studies from Nishikawa and co-workers using single time points provided qualitative support for similar K_ds for Ca^{2+}, Mg^{2+}, and Sr^{2+} under similar solution conditions (*30*).

The k_{max} values for Mg^{2+}, Ca^{2+}, Sr^{2+}, and Ba^{2+} were 3.9, 8.7, 1.5, and 0.069 min^{-1}, respectively (Table 1, Figure 1A). The somewhat larger value of k_{max} for Ca^{2+} than Mg^{2+} is consistent with previous studies (*14*, *31*), although its origin is not understood. Previous studies showed that binding of the structural and catalytic ions is ordered, presumably because binding of the structural ion helps to create the site for the catalytic ion (*20*). Thus, the drop in rate for Sr^{2+} and Ba^{2+} may be because the larger ions, even at saturating concentrations, are unable to induce proper local folding of the ribozyme at the structural site. In addition, Ba^{2+} and Sr^{2+} have the highest pK_As for their aqua ions (*32*), making them especially poor general bases in the classical sense, although k_{max} does not display a monotonic relationship with the pK_A of the aqua ion [13.82, 13.18, 12.70, and 11.42 for Ba^{2+}, Sr^{2+}, Ca^{2+}, and Mg^{2+}, respectively (*32*)], suggesting any underlying metal ion pK_A effect may be hidden.

To test the catalytic site further, we examined the effect of adding transition metal ions to the reaction. In the presence of 10 mM $MnCl_2$ or $CoCl_2$, the rate was appreciable at 0.77 and 0.34 min^{-1}, respectively (Table 2). Zn^{2+} ions were also able to support slow reactivity (0.011 min^{-1}). The effects of Mn^{2+}, Co^{2+}, and Zn^{2+} on the reaction were qualitatively consistent with previous reports (*30*). In contrast, 10 mM Ni^{2+} and Cu^{2+} did not lead to detectable reaction. This may be because these ions tend to interact directly with the bases and may misfold or unfold the ribozyme (*33*).

Reactions were also carried out in the presence of 1 mM $Co(NH_3)_6^{3+}$ and no added divalent ion and revealed no detectable reaction under similar time courses (Table 2). To characterize $Co(NH_3)_6^{3+}$ binding further, the binding affinity of Mg^{2+} was measured in the presence of increasing amounts of $Co(NH_3)_6^{3+}$ (0, 0.1, 1.0, and 10 mM) (Figure 2A, Table 3). $Co(NH_3)_6^{3+}$ and $Mg(H_2O)_6^{2+}$ have similar size and geometry, and $Co(NH_3)_6^{3+}$ is exchange inert, making $Co(NH_3)_6^{3+}$ a good mimic of an outer-sphere metal ion (*34*, *35*). It can be seen that the same k_{max} is reached or approached in the presence of $Co(NH_3)_6^{3+}$ but that $Co(NH_3)_6^{3+}$ increases the concentration of Mg^{2+} required to reach rate saturation. This observation is consistent with previous reports of competitive inhibition by $Co(NH_3)_6^{3+}$ and supports an outer-sphere or weakly dehydrating site for the catalytic ion (*14*). Presumably, $Co(NH_3)_6^{3+}$ is unable to catalyze the reaction because it does not ionize appreciably at pH 7.

The data in this section suggest that this ion is not binding into a region of high charge density. In particular, if an inner-sphere interaction with one or more phosphates was occurring with significant ion desolvation, then one would expect affinity to decrease with ionic radius, as found for the structural ion (see below) (*36*, *37*). Also, it is expected that the K_d for the ion would be significantly smaller (in the micromolar range), especially at low ionic strength, instead of the millimolar range observed here (*27*). In addition, it is expected that the binding affinity would be sensitive to ionic strength, whereas little or no sensitivity has been found (*20*). Thus, our data support this ion either remaining fully hydrated as an outer-sphere or diffuse metal ion or undergoing dehydration but binding into a region of low charge density (*4*). This latter possibility would favor the larger ions, which have smaller enthalpic penalties for dehydration (*32*), as well as provide weak discrimination against Ca^{2+} since Ca^{2+} has a hydration number of 8 and Mg^{2+}, Sr^{2+}, and Ba^{2+} have hydration numbers of 6 (*32*). However, competitive inhibition by $Co(NH_3)_6^{3+}$ suggests that any dehydration is not critical for binding.

Crystallographic studies on the cleaved form of the ribozyme did not reveal a metal ion with high occupancy at the cleavage site, although weak electron density was seen nearby (*11*, *12*). This could arise in part because metal ion

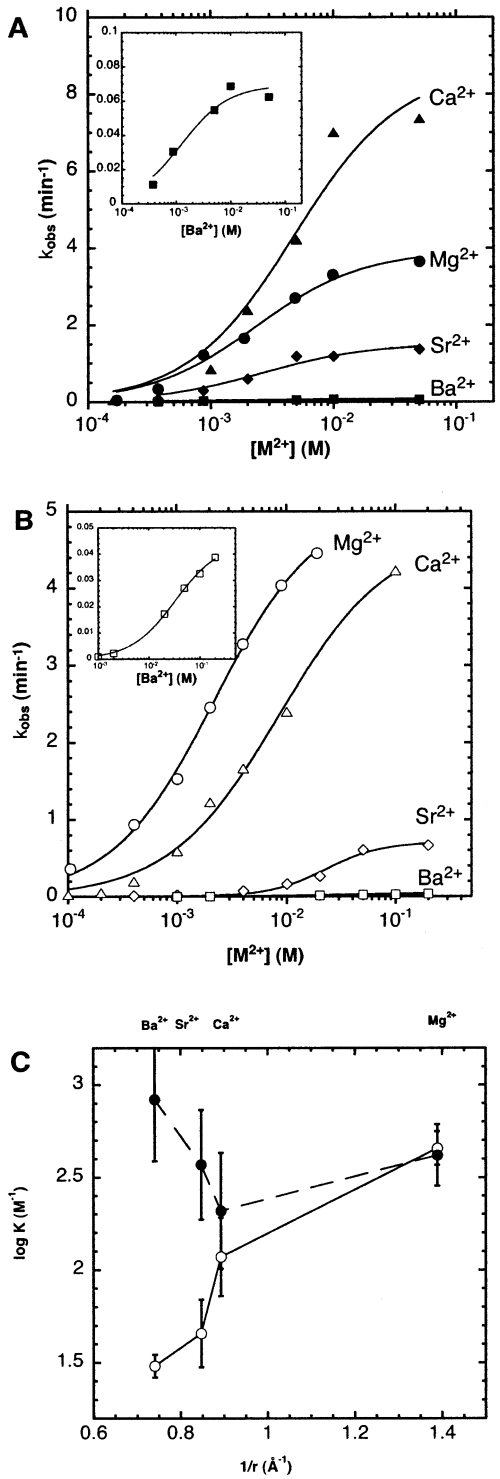

FIGURE 1: Reactivity in the presence of various alkaline earth metal ions. Shown are reactivity−metal profiles at pH 7.0 for Mg^{2+} (circle), Ca^{2+} (triangle), Sr^{2+} (diamond), and Ba^{2+} (square) in 0 M (filled symbols) or 1 M Na^{+} (open symbols). Ba^{2+} data are also given in insets. (A) Data with no added NaCl which probe channel 3 of the mechanism. These data were fit to eq 1a with α_H set to 1. K_d and k_{max} values are given in Table 1. (B) Data with 1 M NaCl which probe channel 2 of the mechanism. These data were fit to the Hill equation (eq 1a). K_d, k_{max}, and α_H values are given in Table 1. (C) Dependence of the log of ion affinity (data from Table 1) on the inverse dehydrated ionic radius for 0 M NaCl (●) and 1 M NaCl (○) conditions. Errors were propagated from values in Table 1 using standard methods (*63*). It is coincidental that the K_d values for Mg^{2+} are identical at the two Na^{+} concentrations at pH 7.0 since two different sites are being probed and because these K_d values are not identical under other pH conditions (*20*).

Table 1: Constants for Divalent Cation Binding to the Ribozyme at pH 7.0

M^{2+}	α_H	$K_{d,Hill}$ (mM)	k_{max} (min^{-1})
0 M NaCl			
Mg^{2+}	1[a]	2.4 ± 0.4	3.9 ± 0.2
Ca^{2+}	1[a]	4.8 ± 1.5	8.7 ± 0.9
Sr^{2+}	1[a]	2.7 ± 0.8	1.5 ± 0.1
Ba^{2+}	1[a]	1.2 ± 0.4	0.069 ± 0.005
1 M NaCl			
Mg^{2+}	0.92 ± 0.06	2.2 ± 0.2	5.1 ± 0.2
Ca^{2+}	0.87 ± 0.095	8.5 ± 1.8	4.7 ± 0.3
Sr^{2+}	1.7 ± 0.4	22 ± 4	0.70 ± 0.05
Ba^{2+}	1[b]	33 ± 2	0.044 ± 0.001

[a] Data were fit with α_H fixed at 1 because 0 M NaCl data were well described by this simpler model (*14*). [b] Insufficient data were available to determine α_H, so its value was fixed at 1.

Table 2: Effect of 1 M NaCl and Various Metal Ions on k_{obs} at pH 7.0

	k_{obs} (min^{-1})	
salt[a]	−NaCl	+1 M NaCl
10 mM Ca^{2+}	7.0 ± 0.4	2.4 ± 0.2
10 mM Mg^{2+}	3.3 ± 0.2	4.0 ± 0.5
10 mM Sr^{2+}	1.2 ± 0.1	0.16 ± 0.01
10 mM Ba^{2+}	0.068 ± 0.002	0.0092 ± 0.0005
10 mM Mn^{2+}	0.77 ± 0.06	3.2 ± 0.1
10 mM Co^{2+}	0.34 ± 0.03	1.4 ± 0.1
10 mM Ni^{2+}	<0.00002	0.029 ± 0.002
10 mM Cu^{2+}	<0.00002	<0.00002
1 mM Zn^{2+}	0.011	3.7 ± 0.1
1 mM Pb^{2+}	nd	0.13 ± 0.01
1 mM $Co(NH_3)_6^{3+}$	<0.00002	0.00063 ± 0.00021
none	<0.00002	0.0010 ± 0.0002

[a] The free concentration of metal ion is provided. For −NaCl conditions, [EDTA] was 0.13 mM, and for +NaCl conditions, [EDTA] was 1 mM to sequester trace ions. For −NaCl conditions, the concentration of metal added was not adjusted for the small amount of EDTA present. For +NaCl conditions, the total concentration of Zn^{2+} and Pb^{2+} was free concentration + 1 mM. Metal chloride was used except for $Pb(OAc)_2$ and $CuSO_4$.

binding is disfavored by the positive charge on a nearby protonated C75 or by a requirement of the scissile phosphate for stronger metal binding, or both. The contribution of the catalytic metal ion to rate acceleration has been found to be modest at ≈25-fold (*20*). This small value is consistent with poor occupancy of this site, as suggested by the crystal structure, and with the pK_A for the aqua ion of a group IIA ion being far removed from neutrality.

Metal Ion Dependence Supports an Inner-Sphere Site for the Structural Ion. The results in the previous section probed the divalent ion dependence of the reaction under low ionic strength conditions. As described in the Background section, experiments at 1 M NaCl and pH 7.0 also gave binding isotherms with α_H equal to 1, and these conditions appear to operate by channel 2 of the mechanism (Scheme 2) in which a structural metal ion stimulates the rate (*20*). As per the previous section, we first looked at the effect of changing Mg^{2+} to other group IIA metal ions. The binding isotherms were reasonably well described by the Hill equation with $\alpha_H \approx 1$ (Table 1, Figure 1B), with the exception of Sr^{2+} which had an α_H of 1.7. The origin of this effect on Sr^{2+} is unclear. (Insufficient data were available to accurately determine α_H for Ba^{2+}, so its value was fixed at 1.)

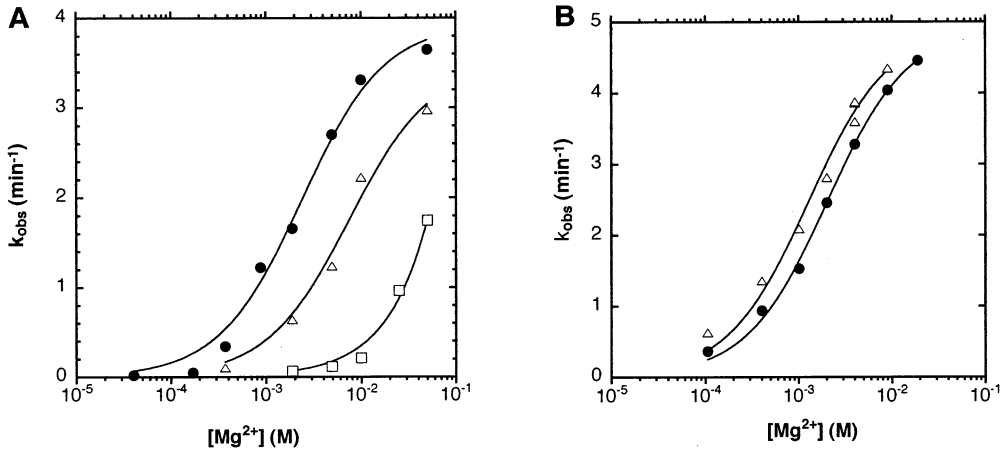

FIGURE 2: Effect of $Co(NH_3)_6^{3+}$ on Mg^{2+} binding to the ribozyme at pH 7.0 in 0 or 1 M Na^+. (A) Data with no added NaCl which probe channel 3 of the mechanism. These data were fit to eq 1a with α_H set to 1. Plots in the absence (●) and presence (△) of 0.1 mM $Co(NH_3)_6^{3+}$ resulted in an observed $K_{d,Mg}$ of 2.4 ± 0.3 mM and 7.4 ± 1.6 mM, respectively, and k_{max} of 3.9 ± 0.2 and 3.5 ± 0.3 min^{-1}, respectively. These values are consistent with competitive inhibition and give a $K_i \approx 48$ μM (=0.1 mM/[(7.4 mM/2.4 mM) − 1]), consistent with the K_i for $Co(NH_3)_6^{3+}$ determined with a Dixon plot (*14*). The rate in the presence of 1 mM $Co(NH_3)_6^{3+}$ is also shown (□); although parameters could not be reliably calculated for this data set, observed binding is significantly weaker under these conditions. (B) Data with 1 M NaCl which probe channel 2 of the mechanism. These data were fit to a binding isotherm for a single ion. Plots in the absence (●) and presence (△) of 0.1 mM $Co(NH_3)_6^{3+}$ resulted in an observed $K_{d,Mg}$ of 2.0 ± 0.1 mM and 1.3 ± 0.2 mM, respectively, and k_{max} of 4.9 ± 0.1 and 4.9 ± 0.2 min^{-1}, respectively. These values are consistent with the absence of $Co(NH_3)_6^{3+}$ competition in 1 M NaCl.

Table 3: Effect of $[Co(NH_3)_6]^{3+}$ on k_{obs} in the Presence of Various Metal Ions and Ionic Strengths

[NaCl] (M)[a]	[$MgCl_2$] added (mM)	$[Co(NH_3)_6]^{3+}$ (mM)	k_{obs} (min^{-1})
1.0	0	0	0.0010 ± 0.0002
1.0	0	0.1	0.00087 ± 0.0001
1.0	0	1.0	0.00063 ± 0.00021
0	10	0	3.3 ± 0.2
0	10	0.1	2.2 ± 0.1
0	10	1.0	0.21 ± 0.01
0	10	10	0.064 ± 0.003
1.0	10	0	4.0 ± 0.5
1.0	10	0.1	4.3 ± 0.3
1.0	10	1.0	5.0 ± 0.2
1.0	10	10	3.5 ± 0.2
1.0	0.2	0	0.36 ± 0.02
1.0	0.2	0.1	0.63 ± 0.06
1.0	0.2	1.0	0.66 ± 0.05

[a] 0 and 1 M NaCl experiments contain 0.13 and 1 mM EDTA, respectively.

Interestingly, the binding affinities for the group IIa metal ions were found to be inversely dependent on ionic radius (Figure 1C). Since log(1/K_d) is proportional to free energy, and 1/r is proportional to Coulombic interaction energy, a positive linear relationship (Figure 1C) is consistent with Coulombic attractions being a major component of the binding (*37*, *38*). As described by Draper and co-workers, this trend can be explained by the Eisenman proposal (*36*, *38*) if the ion is at least partially dehydrated and bound in a location of high charge density (*4*, *37*). This is because although dehydration for a smaller metal ion is more penalizing than for a larger one, smaller metal ions can come into closer contact with phosphate(s), resulting in stronger Coulombic interaction. Curiously, two divalent ion sites were found on a 58-nucleotide fragment of rRNA and showed the same behavior, one site favoring binding of smaller ions and the other weakly discriminating against Ca^{2+} (*37*). Recently, Fang and co-workers performed a similar analysis with group IIA metal ions to argue for inner-sphere coordination of a structural cation to the catalytic domain of RNase P RNA (*39*).

As with the catalytic metal ion, the value of k_{max} decreased significantly for Sr^{2+} and Ba^{2+}, although it was now similar for Mg^{2+} and Ca^{2+} (Table 1, Figure 1B). As suggested in the previous section, the drop in rate for the larger ions may be because these ions, even at saturating concentrations, are unable to induce proper local folding of the ribozyme at the active site. Similarity of k_{max} for Mg^{2+} and Ca^{2+} may be because both ions can fill the structural site in a way to give a similar fold (albeit at slightly different K_ds) and then react without participation of the catalytic ion in the reaction, which has a 2-fold preference for Ca^{2+} (Figure 1A).

Since the structural metal ion site appears to be inner sphere while the catalytic metal ion appears to be outer sphere, it was of interest to test whether $Co(NH_3)_6^{3+}$ could compete under channel 2 conditions. Binding isotherms for Mg^{2+} were measured in no-added and in 0.1 mM $Co(NH_3)_6^{3+}$ (Figure 2B). In contrast to results for the catalytic metal ion, no competition was observed by $Co(NH_3)_6^{3+}$; in fact, a 1.5-fold increase in the affinity of Mg^{2+} was observed under these conditions. Increasing the concentration of $Co(NH_3)_6^{3+}$ further to 1 or 10 mM did not substantially alter k_{obs} in 0, 0.2, or 10 mM Mg^{2+}, as long as 1 M NaCl was present (Table 3). Absence of $Co(NH_3)_6^{3+}$ competition further supports the structural site being inner sphere.

The effect of transition metals on the reaction was also examined under high ionic strength conditions (Table 2). Mn^{2+}, Co^{2+}, and Zn^{2+} (1 or 10 mM) were able to support the reaction at rates similar to that of Mg^{2+}. Although K_d values were not obtained for these ions, the appreciable rate suggests that they are able to bind to the structural metal site with good affinity, also consistent with the ability of these ions to stimulate the reaction in low ionic strength (see above). All three ions have unhydrated radii similar to Mg^{2+} and have a hydration number of 6 (*32*). Pb^{2+}, Ni^{2+}, and Cu^{2+} were not as effective at stimulating the reaction (Table 2),

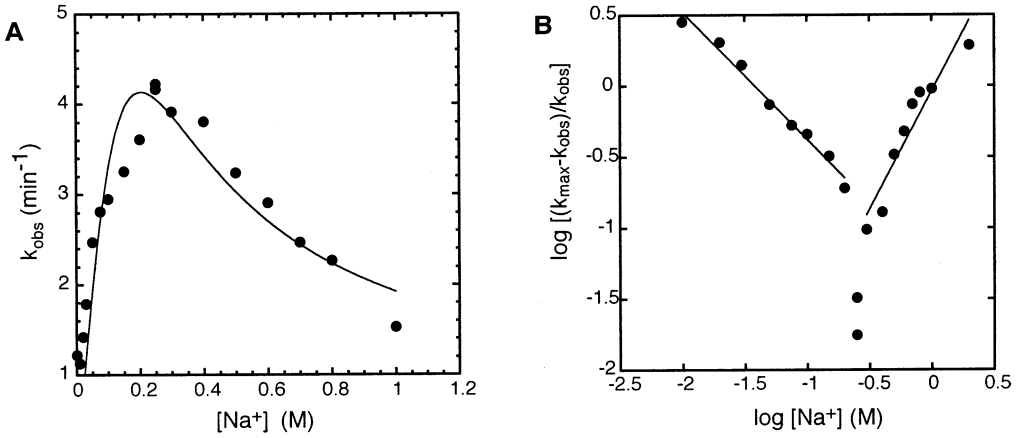

FIGURE 3: (A) Effect of NaCl concentration on k_{obs} in the presence of 1 mM $MgCl_2$/0.13 mM EDTA at pH 7.0. The line is a fit to an equation that assumes an extra channel stimulated by one Na^+ ion (not shown in Scheme 2); although this mechanism gives a fit with a reasonable shape, the molecular nature of the activation portion of the curve is not well understood, and the fitted parameters are therefore not given. (B) Hill plot of Na^+ binding for data in panel A, calculated assuming $k_{max} = 4.3\ min^{-1}$. Slopes of -0.90 ± 0.05 and 1.67 ± 0.23 were obtained for low (10−200 mM) and high (0.3−2 M) NaCl concentration ranges, respectively, and provide estimates of the number of sodium ions taken up by the ribozyme for activation and inhibition, respectively.

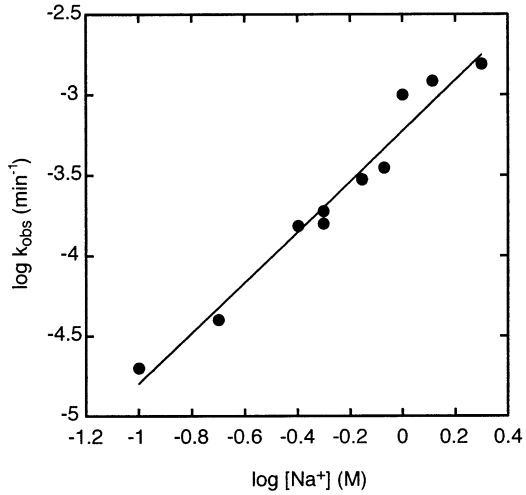

FIGURE 4: Effect of NaCl concentration (0.1−2 M) on k_{obs} in the presence of 1 mM EDTA at pH 7.0 and no added Mg^{2+}. The slope of the line is 1.57 ± 0.10 and provides a lower limit for the number of sodium ions taken up by the ribozyme for channel 1 (eq 6).

again because these ions may misfold or unfold the ribozyme (*33*).

Monovalent Ions Can Compete for Binding of the Structural Ion. Binding of the divalent ion under channel 2 conditions was consistent with an inner-sphere site with a major electrostatic component. Folding and cleavage of the ribozyme can also be achieved in the absence of divalent ions (*14*, *20*), suggesting that monovalent ions may also be able to fill this site. To explore this possibility, we measured the effect on k_{obs} of increasing monovalent ion concentration in the presence of 1 mM Mg^{2+}. As shown in Figure 3A, k_{obs} displays a bell-shaped dependence on NaCl concentration with a maximum near 0.2 M NaCl. The ion dependence of these two phases was analyzed by a Hill plot (eq 1b) (Figure 3B). At lower NaCl concentrations, an α_H of 0.90 ± 0.05 was obtained, consistent with a stimulatory effect upon net uptake of one ion. At higher NaCl concentrations, an α_H of -1.67 ± 0.23 was obtained, consistent with an inhibitory effect upon net uptake of two ions.

The stimulatory effect below ≈200 mM NaCl, which is near physiological ionic strength (*32*), may be due to stimulation of RNA folding. We have observed similar effects on the folding of the ribozyme during transcription (*40*), and others have reported similar phenomena for folding of a group I intron (*41*−*44*). The basis for stimulation by NaCl appears to be a complex mixture of effects on tertiary structure destablization (see below) and on secondary structure (data not shown) and will be described elsewhere.

The slope of 1.7 at higher Na^+ concentration (Figure 3B) suggests that ≈2 monovalent ions are taken up by the ribozyme, leading to a less reactive state. Prior dissection of the folding of the ribozyme in metal-buffered experiments revealed a divalent ion-independent channel for the reaction (channel 1 of Scheme 2) (*20*). The inhibition by Na^+ can be explained within the context of the three-channel model wherein two Na^+ ions displace one structural Mg^{2+} ion from its binding site and place the reaction into the slower reacting channel 1 (the rate of which was not measured in this experiment). That two Na^+ ions are required for displacement of one Mg^{2+} ion is consistent with such a site having a significant electrostatic component, possibly involving coordination to two phosphate ions.

These data predict that two Na^+ ions might also be required for activation of the ribozyme in the *absence* of divalent ions. A plot of log k_{obs} versus NaCl concentration in the absence of added divalent metal ion (Figure 4) gave a slope of 1.57 ± 0.10 and was linear from 2 M down to the lowest NaCl concentration tried of 100 mM. As described by eq 6, this is consistent with the uptake of two Na^+ ions for divalent ion-independent reactivity, in accord with Scheme 2.

The K_{d,Na^+} for inhibition by Na^+ can be qualitatively assessed from these data. The increase in k_{obs} through 2 M NaCl in the absence of Mg^{2+} (Figure 4) (possibly beginning to level off above 1 M) suggests that Na^+ is binding very weakly and the apparent K_d is in the molar range. Likewise, requirement of ≈300 mM Na^+ to inhibit 1 mM Mg^{2+} (Figure 3) also suggests that the K_{d,Na^+} is in this range. Weak binding of Na^+ can be understood in the greater entropy loss for binding of two Na^+ ions versus one Mg^{2+} ion (although this is partially offset by the high concentration of NaCl) and in the potential repulsion between the two nearby Na^+ ions.

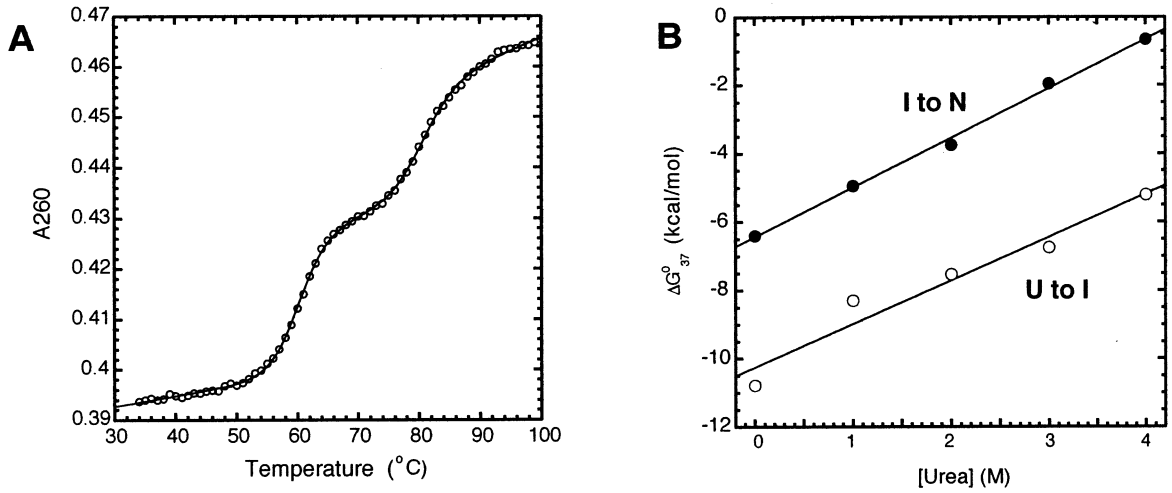

FIGURE 5: Effect of urea on the melting profile of the cleaved ribozyme. (A) Melting profile in 0.1 mM Mg^{2+}/25 mM HEPES (pH 8.0). Data were fit (solid line) to a three-state model as described in the text (see Table 4). (B) Determination of *m*-values (slope) from UV melting data for the I to N transition (●) (*m*-value of 1.45 ± 0.05 kcal mol^{-1} M^{-1}, $r^2 = 0.997$) and U to I transition (○) (*m*-value of 1.27 ± 0.17 kcal mol^{-1} M^{-1}, $r^2 = 0.948$) in 0.1 mM Mg^{2+}/25 mM HEPES (pH 8.0).

Table 4: Thermodynamic Parameters for Folding of the Ribozyme in 0.1 mM Mg^{2+} as a Function of Urea Concentration[a]

[urea] (M)	$-\Delta H°_1$ (kcal mol^{-1})	$T_{M,1}$ (°C)	$-\Delta S°_1$ (eu)	$-\Delta G°_{37,1}$ (kcal mol^{-1})	m_1 (kcal mol^{-1} M^{-1})	$-\Delta H°_2$ (kcal mol^{-1})	$T_{M,2}$ (°C)	$-\Delta S°_2$ (eu)	$-\Delta G°_{37,2}$ (kcal mol^{-1})	m_2 (kcal mol^{-1} M^{-1})
0	92.1	60.2	276.2	6.4	1.45 ± 0.05	87.5	80.6	247.5	10.8	1.27 ± 0.17
1	91.4	54.7	278.9	4.9		71.0	78.0	202.1	8.3	
2	89.4	50.6	276.1	3.7		68.1	75.6	195.3	7.5	
3	74.2	45.4	232.8	2.0		65.8	72.4	190.5	6.7	
4	79.1	39.6	252.9	0.7		53.8	70.3	156.6	5.2	

[a] Parameters for transition 1 (subscript 1) correspond to the I to N transition for secondary to tertiary structure, while the parameters for transition 2 (subscript 2) correspond to the U to I for primary to secondary transition. Errors in $\Delta H°$ and $\Delta S°$ are estimated at 10% on the basis of fitting, while errors in $\Delta G°_{37}$ and T_M are estimated at 5% and 1 °C, respectively, and are smaller than for $\Delta H°$ and $\Delta S°$ due to correlation of $\Delta H°$ and $\Delta S°$ (*62*).

Interestingly, the binding of Na^+ ions to the cleaved form of the ribozyme appears to be substantially tighter (see below), suggesting that the tertiary structure may be less stable for the precursor ribozyme.

Melting Experiments Identify Tertiary and Secondary Structure Unfolding Steps. Large RNAs with tertiary structure typically melt in a hierarchical fashion, with tertiary structure melting before requisite and independently stable secondary structure (*45*−*47*). Unfolding of the HDV ribozyme cleavage product was examined, and two major unfolding transitions were observed (Figure 5), in agreement with prior melting studies on the genomic product (*48*). In an effort to assign the first transition, we examined the urea dependence of melting. These experiments were conducted at pH 8 in order to separate the two transitions further. This appears to occur because of deprotonation of a quartet involving C41 (*48*). As described in the Materials and Methods section, the data were fit with a three-state model involving two coupled equilibria (Scheme 3). A typical melt and fit are shown in Figure 5A, the resulting *m*-value plots are in Figure 5B, and thermodynamic parameters are in Table 4. Plots of free energy for the I to N and U to I transitions versus urea concentration were linear with slopes of 1.45 ± 0.05 and 1.27 ± 0.17, respectively.

As described by Shelton et al., the *m*-value is proportional to the amount of surface area buried in the folding transition and holds for both RNA secondary and tertiary structure transitions (*28*). This is similar to the case for protein folding (*49*). The *m*-value of 1.45 ± 0.05 for tertiary folding (I to N) can be compared with that for $tRNA^{Phe}$. Both RNAs have approximately the same number of nucleotides in their tertiary structures and therefore likely bury approximately the same amount of surface area in folding from secondary to tertiary structure. Similar amounts of tertiary structure are also supported by recent calculations (*9*). Both titrations of Mg^{2+} at fixed urea concentration and of urea at fixed Mg^{2+} concentration have been used to obtain an *m*-value of 1.7 ± 0.1 for $tRNA^{Phe}$. This *m*-value compares well to the value of 1.45 for the HDV ribozyme. The *m*-value for $tRNA^{Phe}$ was shown to be independent of Mg^{2+} concentration between 0.1 and 0.5 mM (*28*), suggesting that the value obtained here in 0.1 mM Mg^{2+} is directly comparable. (The small discrepancy in *m*-values may be because the C41 quartet is partially unfolded at pH 8, resulting in somewhat less surface area burial.) This result supports assignment of the first folding transition to tertiary structure. This comparison also suggests that *m*-values can be obtained by thermal denaturation and provides a good way to judge the extent of tertiary structure folding.

An *m*-value was also calculated for the first unfolding transition in the presence of 100 mM Na^+ (data not shown). Unfortunately, the fit to the simple two transition model in Scheme 3 was not as good as for 0.1 mM Mg^{2+}; the average χ^2 across all urea values was nearly 10 times higher in 100 mM Na^+ than 0.1 mM Mg^{2+}. This precluded an *m*-value from being obtained for this transition in NaCl.

An *m*-value was also calculated for the transition for secondary structure formation (U to I) in 0.1 mM Mg^{2+}. This

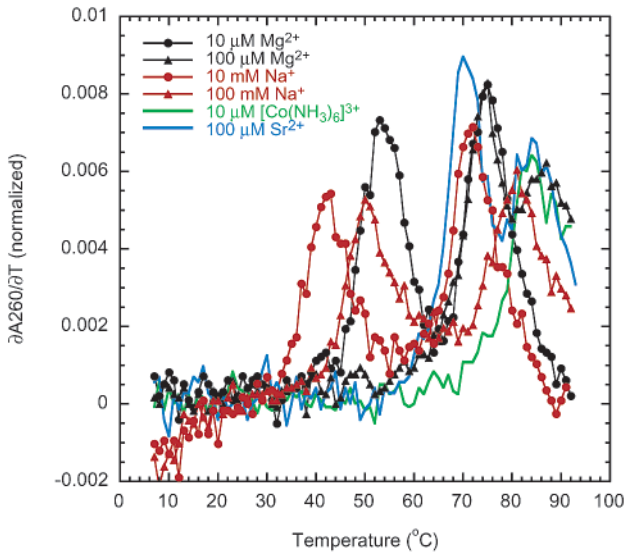

FIGURE 6: Melting profiles for the cleaved ribozyme in the presence of various metal ions. Melting was at 260 nm in 25 mM HEPES (pH 7.0) with the following salts: $MgCl_2$, NaCl, $SrCl_2$, or $Co(NH_3)_6Cl_3$. Concentrations and symbols are provided in the figure.

m-value is subject to greater error than the first because of the difficulty of obtaining a good upper baseline at low urea concentrations, the possibility of backbone hydrolysis contributing to the change, and the simplifying assumption that all secondary structure unfolds in a single transition. An *m*-value of 0.94 was obtained for secondary structure formation by $tRNA^{Phe}$, which was also assumed to form in a single step (*28*). Unfolding of $tRNA^{Phe}$ secondary structure involves breaking of 21 bp, while unfolding of HDV tertiary structure breaks 28 bp. (This count excludes P1.1 and the AG base pair at the top of P4, both of which likely require tertiary structure to form.) Correction of the *m*-value of 0.94 gives a value of 1.25, which is in good agreement with the value of 1.27 obtained here.

The *m*-values obtained support assignment of the melting transitions to tertiary structure followed by secondary structure, as expected from the hierarchical model for RNA folding (*46*). These experiments help to rule out other possibilities for the two transitions, such as melting out of two different secondary structures or an optically silent melting out of tertiary structure.

Ion Dependence of Tertiary Unfolding Supports an Inner-Sphere Structural Ion. The effect of metal ion identity and concentration on the two melting transitions was examined. Both the first and second melting transitions were stabilized by increasing concentrations of Mg^{2+} from 10 to 100 μM (Figure 6). Melts in 10 and 100 mM Na^+ also revealed two transitions, with both transitions stabilized by increasing Na^+ concentration (Figure 6). The first transition in Mg^{2+} was assigned to tertiary structure from the *m*-value plots, but this could not be done for Na^+ (see previous section). However, experiments from Been and co-workers, in 400 mM NaCl involving mutations of the C41 quartet, clearly showed that the first transition in Na^+ is due to tertiary structure as well (*48*). [Note that the T_M for the first transition in 100 mM Na^+ of ≈50 °C (Figure 6) is consistent with the reported value of ≈65 °C in higher Na^+ of 400 mM (*48*).] The ability of Na^+ to stabilize the tertiary structure of the ribozyme is expected from the divalent ion-independent channel in Scheme 2.

Interestingly, 10 μM $Co(NH_3)_6^{3+}$ gave rise to only one melting transition, with a T_M approximately equal to the second T_M for 100 μM divalent ions (Figure 5). This suggests that $Co(NH_3)_6^{3+}$ does not give rise to a stable tertiary structure and supports the notion that tertiary structure is stabilized by an inner-sphere ion. [It is unlikely that both the secondary and tertiary structures melt in this transition since the sharpness of the transition as assessed by the first derivative is the same as the secondary structure transition in Mg^{2+}, Sr^{2+}, and Na^+ (Figure 6).] Although 100 μM Sr^{2+} gave rise to two transitions, it was less effective than 100 μM Mg^{2+} at stabilizing the tertiary unfolding (ΔT_M ≈5 °C), consistent with ion selectivity for the tertiary unfolding.

Affinity and Stoichiometry of Ion Binding to the Cleaved Ribozyme. An inner-sphere binding site is present only once an RNA folds into its tertiary structure. One diagnostic for such a site is the dependence of the melting temperature of the tertiary structure on metal ion concentration. If binding sites for the ion(s) are present in both the folded and unfolded sites, then the T_M will level off at high ion concentrations since the transition will be between metal-bound states. However, if the metal ion site is present only in the folded state, the T_M will increase indefinitely with metal ion concentration (see Materials and Methods) (*27*). We first examined the relationship between T_M and Na^+ in the absence of added divalent ions. These experiments were conducted at pH 7.0 to help to reduce RNA hydrolysis at high temperatures. As indicated in the Materials and Methods section, many of these melts could not be fit to the three-state model due to the absence of a good upper baseline. In these cases, the two transitions generally remained well separated, and the T_Ms were estimated from the first derivatives.

As shown in Figure 7A, the T_Ms for the two transitions were well resolved at all Na^+ concentrations. A plot of inverse T_M versus log [Na^+] shows a linear decrease up to the highest concentration attempted of 1.5 M. This profile is consistent with these Na^+ ions binding primarily to the tertiary structure and not the secondary structure. [The point at 2 mM Na^+ is above the plateau region of the plot (Figure 7B) and is similar to that at extremely low Mg^{2+} concentrations (Figure 8), suggesting that the RNA is not folded under these conditions; this data point was not used in the analysis.] Fitting to eqs 15 and 17 returned 1.5 ± 0.1 ions binding with an affinity, K_{d,Na^+}, of 15 mM (Figure 7). [ΔH_0 in eq 15 was determined at 10 mM Na^+ using a fit according to Scheme 3 (data not shown); 10 mM Na^+ is in the plateau region of the curve (Figure 7B), suggesting the RNA is folded but without significant occupancy of the binding site.] The value of 1.5 ions is similar to Hill constants obtained for reaction of the precursor ribozyme (Figures 3 and 4), supporting stabilization of the tertiary structure by Na^+.

Next, we examined the effect of Mg^{2+} on the T_M in the presence and absence of 100 mM Na^+. Data in the background of 100 mM Na^+ supported Mg^{2+} binding to a stable tertiary structure on the basis of the absence of a sigmoidal curve. These data were fit to eqs 15 and 17 using the same ΔH_0 and returned a value of 1.15 ± 0.05 ions binding with an affinity, $K_{d,str}$, of 21 μM (Figure 8). This ion is tentatively assigned to the structural ion rather than

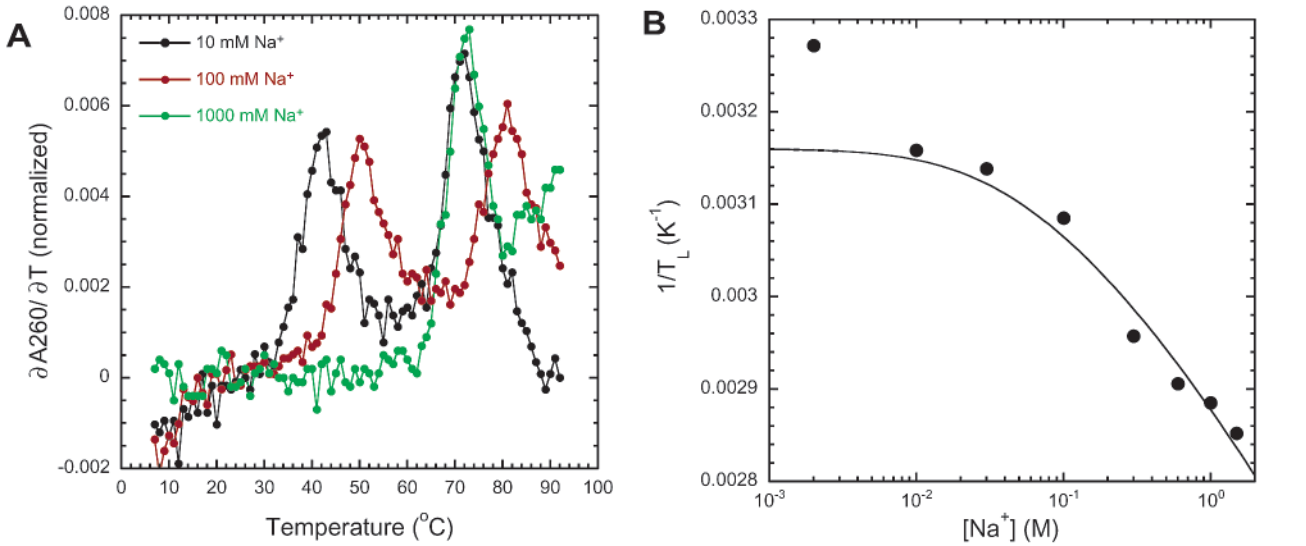

FIGURE 7: Effect of NaCl concentration on the melting temperature for the cleaved ribozyme at pH 7.0. (A) Melting curves for the wild-type ribozyme in 0.01 M (black), 0.1 M (red), and 1 M NaCl (green). The two transitions are well separated in all cases. (B) Dependence of T_L, the T_M in the presence of ligand, on Na^+ concentration for the first transition. The fit (solid line) is from eqs 15 and 17 using a ΔH_0 of 62.2 kcal/mol (from a three-state fit in 10 mM Na^+) and a T_0 of 43.3 °C and resulted in 1.5 ± 0.1 Na^+ ions bound to the ribozyme with an apparent K_d of 14.5 ± 4.5 mM. The point at 2 mM Na^+ was excluded from the fit.

the catalytic one on the basis of the similarities between the ion-stabilizing characteristics of this melting transition and that of channel 2 of the reaction (Figures 1, 2, and 6). The catalytic site may not be sensed in this experiment since it appears to be a low-affinity site and may require the scissile phosphate to form.

Data for Mg^{2+} binding in the absence of added Na^+ are distinctly sigmoidal (Figure 8). However, we are hesitant to interpret the shape of this curve in detail for several reasons: folding and metal ion binding may be coupled at low Mg^{2+} concentrations in the absence of NaCl, a good unfolding baseline could not be obtained at higher Mg^{2+} concentrations, and hydrolysis of the RNA is likely to be significant at the high melting temperatures. Nevertheless, a few qualitative conclusions can be drawn. First, the tertiary structure is extraordinarily stable in 1 mM Mg^{2+} with an apparent T_M of 85 °C or more. Second, although the data prevent $K_{d,str}$ from being obtained, the downward curvature of the plot starting at 0.1 μM suggests that Mg^{2+} binds very tightly in the absence of Na^+. Third, Na^+ destabilizes the tertiary structure in the presence of Mg^{2+} (compare the data between 10 μM and 1 mM Mg^{2+} in Figure 8), consistent with the competitive behavior inferred from cleavage studies on the precursor (Scheme 2). Competition of Na^+ for binding of Mg^{2+} has been shown in many systems, including the P4−P6 domain of the *Tetrahymena* ribozyme (*44*).

It is of interest to consider several implications of the data in Figures 7 and 8. First, the K_d for the structural Mg^{2+} ion measured in 1 M NaCl from activity studies on the precursor RNA is 2.2 mM (Table 1, Figure 1B). Application of eq 8 and the value of K_{d,Na^+} from Figure 7 returns an intrinsic binding constant for the structural Mg^{2+} ion of $K_{d,str} \approx 0.53$ μM. This value is in agreement with the quasi-binding constant obtained from the downward curvature of the Mg^{2+}-only plot in Figure 8. These data also support the assumption that the structural site is filled and the ribozyme already folded at the hundred micromolar divalent ion concentrations required to obtain onset of activity at low ionic strength

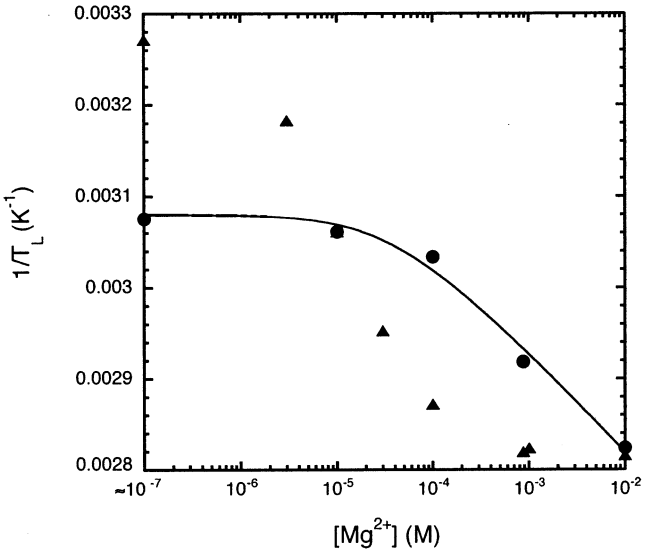

FIGURE 8: Effect of $MgCl_2$ concentration on the melting temperature for the cleaved ribozyme at pH 7.0 in the presence (●) and absence (▲) of 100 mM Na^+. The fit (solid line) is to 100 mM Na^+ data from eqs 15 and 17 using a $\Delta H°$ of 62.2 kcal/mol (from a three-state fit in 10 mM Na^+) and a T_0 of 51.5 °C and resulted in 1.15 ± 0.05 Mg^{2+} ions bound to the ribozyme with an apparent K_d of 20.8 ± 7.2 μM. The no-added Na^+ data were not fit since folding and metal binding may be coupled at low Mg^{2+} concentration in the absence of Na^+, and hydrolysis of the RNA may be problematic due to the high T_M at high Mg^{2+} concentrations. The point labeled "≈10^{-7}" is from a melt with 1 mM EDTA and no added Mg^{2+}. The concentration of 10^{-7} is approximate for contaminating divalent ions and is based on our previous study (*20*). The actual value is not critical to the interpretation of the data since the curve is level between this value and 10 μM Mg^{2+}.

conditions (Figure 1A). Moreover, application of $K_{d,str} \approx 0.53$ μM and eq 8 at 0.1 M Na^+ returns a $K_{d,app}$ for the structural ion of 25 μM in 0.1 M Na^+, in good agreement with the observed value of 21 μM from melting experiments (Figure 8). Thus, these data provide consistency across the activity experiments on the precursor ribozyme and the thermodynamic experiments on the self-cleaved ribozyme.

The tertiary fold of the cleaved ribozyme appears to be unusually stable. This is evidenced by a T_M greater than 85 °C in 10 mM Mg^{2+} and of ≈40 °C in only 10 mM Na^+ (Figure 6). Indeed, melting data at 100 mM Na^+ (Figure 6) and K_{d,Na^+} suggest that essentially all of the ribozyme should be folded at 37 °C, the temperature at which the kinetics were measured. On the basis of this, the expectation is that the rate for channel 1 should level off with Na^+ concentration around 50−100 mM. However, this does not occur; k_{obs} for the precursor ribozyme increases with NaCl concentrations beyond 1 M (Figure 4). Moreover, data in the presence of NaCl were consistent with a model wherein 1 M NaCl is able to induce <1% of the precursor ribozyme molecules into the proper tertiary structure fold (*20*). These data suggest that the tertiary structure of the precursor is substantially less stable than that of the cleaved ribozyme. It is worth speculating why this might be.

The precursor ribozyme is subject to numerous misfolds containing different alternative pairings of the secondary structure (*25*). In particular, even the fast-folding G11C mutant studied herein is subject to the Alt 3 misfold. Thus, some of the apparent loss in tertiary stability of the precursor may be because the ribozyme is misfolded. This less interesting possibility cannot be ruled out at this time. Alternatively (or in addition), the reactive precursor ribozyme may assume a number of ground state interactions that destabilize the tertiary fold. [Note that mechanistic data thus far support the active form of the HDV precursor ribozyme being similar to the crystal structure of the cleaved form, including P1.1 (*50*, *51*).] Such interactions might include anticooperative interaction between proton and metal binding (*14*), placement of the scissile phosphate into a region of high negative potential (*11*, *20*), or driving a nucleobase into an unusual tautomeric state, as has been suggested for the hairpin ribozyme (*52*). A quasi-stable precursor ribozyme would also be consistent with the unfavorable activation entropy and conformational change for HDV ribozyme cleavage measured by Walter and co-workers (*53*). A similar scenario of a partially folded ground state has been proposed in the mechanism of the hammerhead ribozyme (*54*). Unfavorable interactions in the ground state can provide a driving force for catalysis, assuming they are relieved in the transition state (*55*).

CONCLUSIONS

The experiments herein support two distinct classes of metal ions on the HDV ribozyme: an outer-sphere ion involved as the general base in the reaction and an inner-sphere ion involved in a structural role. The outer-sphere ion is supported by insensitivity of binding affinity to dehydrated ionic radius and by competition by $Co(NH_3)_6^{3+}$ but not Na^+. The inner-sphere ion is supported by increase of binding affinity with decrease in dehydrated ionic radius and by competition by Na^+ but not $Co(NH_3)_6^{3+}$. This holds for both functional studies on the precursor ribozyme and thermodynamic studies on the cleaved ribozyme. In addition, the intrinsic affinity of the inner-sphere ion is unusually high, and its T_M has the dependence on metal ion concentration expected for binding to a folded RNA with tertiary structure.

The high affinity of the structural Mg^{2+} ion in low ionic strength ($K_{d,str} \approx 0.5\ \mu M$) is similar to the tightest Mg^{2+} ion binding constants measured for $tRNA^{Phe}$ in low ionic strength (*6*). However, there is not a clear correlation between this affinity and a specific ion in $tRNA^{Phe}$, precluding any attempt at identifying the structural ion in HDV by comparison. Several divalent ions were found in the crystal structure of the ribozyme (*11*, *12*), and roles for divalent ions have been implicated from functional studies on the ribozyme (*56*−*58*). The present data do not speak to which, if any, of these ions is the critical structural ion being observed. Several of the crystallographic ions are in regions of high negative potential (*20*), as expected from theoretical considerations (*59*−*61*), and it remains likely that the inner-sphere site will be near one of these regions. It will be of interest to try to identify the binding site of this ion using structure−function correlation under the appropriate channel conditions.

ACKNOWLEDGMENT

We thank members of the Bevilacqua laboratory for critical comments on the manuscript.

REFERENCES

1. Rialdi, G., Levy, J., and Biltonen, R. (1972) *Biochemistry 11*, 2472−2479.
2. Romer, R., and Hach, R. (1975) *Eur. J. Biochem. 55*, 271−284.
3. Reid, B. R., and Robillard, G. T. (1975) *Nature 257*, 287−291.
4. Gluick, T. C., Wills, N. M., Gesteland, R. F., and Draper, D. E. (1997) *Biochemistry 36*, 16173−16186.
5. Nixon, P. L., and Giedroc, D. P. (1998) *Biochemistry 37*, 16116−16129.
6. Misra, V. K., and Draper, D. E. (1998) *Biopolymers 48*, 113−135.
7. Basu, S., Rambo, R. P., Strauss-Soukup, J., Cate, J. H., Ferre-D'Amare, A. R., Strobel, S. A., and Doudna, J. A. (1998) *Nat. Struct. Biol. 5*, 986−992.
8. Correll, C. C., Wool, I. G., and Munishkin, A. (1999) *J. Mol. Biol. 292*, 275−287.
9. Conn, G. L., Gittis, A. G., Lattman, E. E., Misra, V. K., and Draper, D. E. (2002) *J. Mol. Biol. 318*, 963−973.
10. Shih, I. H., and Been, M. D. (2002) *Annu. Rev. Biochem. 71*, 887−917.
11. Ferre-D'Amare, A. R., Zhou, K., and Doudna, J. A. (1998) *Nature 395*, 567−574.
12. Ferre-D'Amare, A. R., and Doudna, J. A. (2000) *J. Mol. Biol. 295*, 541−556.
13. Perrotta, A. T., Shih, I., and Been, M. D. (1999) *Science 286*, 123−126.
14. Nakano, S., Chadalavada, D. M., and Bevilacqua, P. C. (2000) *Science 287*, 1493−1497.
15. Muth, G. W., Ortoleva-Donnelly, L., and Strobel, S. A. (2000) *Science 289*, 947−950.
16. Rupert, P. B., and Ferre-D'Amare, A. R. (2001) *Nature 410*, 780−786.
17. Nakano, S., and Bevilacqua, P. C. (2001) *J. Am. Chem. Soc. 123*, 11333−11334.
18. Oyelere, A. K., Kardon, J. R., and Strobel, S. A. (2002) *Biochemistry 41*, 3667−3675.
19. Luptak, A., Ferre-D'Amare, A. R., Zhou, K., Zilm, K. W., and Doudna, J. A. (2001) *J. Am. Chem. Soc. 123*, 8447−8452.
20. Nakano, S., Proctor, D. J., and Bevilacqua, P. C. (2001) *Biochemistry 40*, 12022−12038.
21. Shih, I. H., and Been, M. D. (2001) *Proc. Natl. Acad. Sci. U.S.A. 98*, 1489−1494.
22. Thompson, J. E., and Raines, R. T. (1994) *J. Am. Chem. Soc. 116*, 5467−5468.
23. Zhou, J. M., Zhou, D. M., Takagi, Y., Kasai, Y., Inoue, A., Baba, T., and Taira, K. (2002) *Nucleic Acids Res. 30*, 2374−2382.
24. Chadalavada, D. M., Knudsen, S. M., Nakano, S., and Bevilacqua, P. C. (2000) *J. Mol. Biol. 301*, 349−367.
25. Chadalavada, D. M., Senchak, S. E., and Bevilacqua, P. C. (2002) *J. Mol. Biol. 317*, 559−575.
26. Draper, D. E., Bukhman, Y. V., and Gluick, T. C. (2000) in *Current Protocols in Nucleic Acid Chemistry* (Beaucage, S. L.,

Bergstrom, D. E., Glick, G. D., and Jones, R. A., Eds.) pp 11.3.1−11.3.13, John Wiley & Sons, New York.
27. Laing, L. G., Gluick, T. C., and Draper, D. E. (1994) *J. Mol. Biol. 237*, 577−587.
28. Shelton, V. M., Sosnick, T. R., and Pan, T. (1999) *Biochemistry 38*, 16831−16839.
29. Schellman, J. A. (1975) *Biopolymers 14*, 999−1018.
30. Suh, Y. A., Kumar, P. K., Taira, K., and Nishikawa, S. (1993) *Nucleic Acids Res. 21*, 3277−3280.
31. Shih, I. H., and Been, M. D. (1999) *RNA 5*, 1140−1148.
32. Feig, A. L., and Uhlenbeck, O. (1999) in *The RNA World* (Gesteland, R. F., Cech, T. R., and Atkins, J. F., Eds.) 2nd ed., pp 287−319, Cold Spring Harbor Laboratory Press, Cold Spring Harbor, NY.
33. Saenger, W. (1984) *Principles of Nucleic Acid Structure*, Springer-Verlag, New York.
34. Basolo, R., and Pearson, R. G. (1988) *Mechanisms of Inorganic Reactions*, John Wiley & Sons, New York.
35. Suga, H., Cowan, J. A., and Szostak, J. W. (1998) *Biochemistry 37*, 10118−10125.
36. Eisenman, G., and Horn, R. (1983) *J. Membr. Biol. 76*, 197−225.
37. Bukhman, Y. V., and Draper, D. E. (1997) *J. Mol. Biol. 273*, 1020−1031.
38. Eisenman, G. (1962) *Biophys. J. 2*, 259−323.
39. Fang, X. W., Thiyagarajan, P., Sosnick, T. R., and Pan, T. (2002) *Proc. Natl. Acad. Sci. U.S.A. 99*, 8518−8523.
40. Diegelman-Parente, A., and Bevilacqua, P. C. (2002) *J. Mol. Biol. 324*, 1−16.
41. Silverman, S. K., Deras, M. L., Woodson, S. A., Scaringe, S. A., and Cech, T. R. (2000) *Biochemistry 39*, 12465−12475.
42. Heilman-Miller, S. L., Pan, J., Thirumalai, D., and Woodson, S. A. (2001) *J. Mol. Biol. 309*, 57−68.
43. Russell, R., Zhuang, X., Babcock, H. P., Millett, I. S., Doniach, S., Chu, S., and Herschlag, D. (2002) *Proc. Natl. Acad. Sci. U.S.A. 99*, 155−160.
44. Uchida, T., He, Q., Ralston, C. Y., Brenowitz, M., and Chance, M. R. (2002) *Biochemistry 41*, 5799−5806.
45. Laing, L. G., and Draper, D. E. (1994) *J. Mol. Biol. 237*, 560−576.
46. Brion, P., and Westhof, E. (1997) *Annu. Rev. Biophys. Biomol. Struct. 26*, 113−137.
47. Tinoco, I., Jr., and Bustamante, C. (1999) *J. Mol. Biol. 293*, 271−281.
48. Wadkins, T. S., Shih, I., Perrotta, A. T., and Been, M. D. (2001) *J. Mol. Biol. 305*, 1045−1055.
49. Myers, J. K., Pace, C. N., and Scholtz, J. M. (1995) *Protein Sci. 4*, 2138−2148.
50. Wadkins, T. S., Perrotta, A. T., Ferre-D'Amare, A. R., Doudna, J. A., and Been, M. D. (1999) *RNA 5*, 720−727.
51. Nishikawa, F., and Nishikawa, S. (2000) *Nucleic Acids Res. 28*, 925−931.
52. Pinard, R., Hampel, K. J., Heckman, J. E., Lambert, D., Chan, P. A., Major, F., and Burke, J. M. (2001) *EMBO J. 20*, 6434−6442.
53. Pereira, M. J., Harris, D. A., Rueda, D., and Walter, N. G. (2002) *Biochemistry 41*, 730−740.
54. Peracchi, A., Karpeisky, A., Maloney, L., Beigelman, L., and Herschlag, D. (1998) *Biochemistry 37*, 14765−14775.
55. Jencks, W. P. (1975) *Adv. Enzymol. 43*, 219−410.
56. Lafontaine, D. A., Ananvoranish, S., and Perreault, J.-P. (1999) *Nucleic Acids Res. 27*, 3236−3243.
57. Ananvoranich, S., and Perreault, J. P. (2000) *Biochem. Biophys. Res. Commun. 270*, 600−607.
58. Tanaka, Y., Hori, T., Tagaya, M., Sakamoto, T., Kurihara, Y., Katahira, M., and Uesugi, S. (2002) *Nucleic Acids Res. 30*, 766−774.
59. Misra, V. K., and Draper, D. E. (1999) *J. Mol. Biol. 294*, 1135−1147.
60. Misra, V. K., and Draper, D. E. (2000) *J. Mol. Biol. 299*, 813−825.
61. Misra, V. K., and Draper, D. E. (2002) *J. Mol. Biol. 317*, 507−521.
62. SantaLucia, J., Jr., and Turner, D. H. (1997) *Biopolymers 44*, 309−319.
63. Bevington, P. R. (1969) *Data Reduction and Error Analysis for the Physical Sciences*, McGraw-Hill, New York.

BI026815X